ELSEVIER

Biophysical Chemistry 126 (2007) 80–85

Biophysical Chemistry

http://www.elsevier.com/locate/biophyschem

Low-frequency normal modes in horse liver alcohol dehydrogenase and motions of residues involved in the enzymatic reaction

Jia Luo, Thomas C. Bruice *

Department of Chemistry, University of California at Santa Barbara, Santa Barbara, CA 93106, United States

Received 1 March 2006; accepted 10 May 2006
Available online 5 June 2006

Abstract

Normal mode analysis using the elastic network model has provided characteristics and directions of the low-frequency large domain motions of horse liver alcohol dehydrogenase. Three normal modes (mode 1, mode 7, and mode 8) were identified as representative domain motions that may promote the onset of Near Attack Conformers or facilitate the product to be released. The pattern of the atomic displacement for some key residues (such as Val292 and Val203) revealed in this study is in line with experimental structural and kinetic studies and theoretical simulations.

Keywords: Normal mode analysis; Horse liver alcohol dehydrogenase

1. Introduction

Horse liver alcohol dehydrogenase (HLADH, EC 1.1.1.1) [1] has a molecular weight of 80,000 Da and is a dimer of two identical subunits [2]. Each subunit binds a nicotinamide coenzyme and two Zn(II) ions. One zinc is in the active site, while the other is structural. The active site Zn(II) is associated with the hydroxyl oxygen of the alcohol substrate. Complexation of the oxygen of the substrate alcohol by Zn^{2+} lowers the pK_a of the alcohol hydroxyl group. Dissociation of the alcohol hydroxyl proton is the first step in the oxidation of alcohol by NAD^+ (Eq. (1)). This proton is passed to water by

$$\{E–NAD^+–RCH_2OH\} \rightleftharpoons \{E–NAD^+–RCH_2O^-\} + H^+ \quad (1)$$

$$\{E–NAD^+–RCH_2O^-\} \rightleftharpoons \{E–NADH–RCHO\} \quad (2)$$

way of a hydrogen-bond network terminating with the imidazole of His51 [3,4]. The second step of the reaction involves hydride equivalent transfer from the alkoxide to NAD^+ [5,6] (Eq. (2)).

A common feature in the structures of certain dehydrogenases is the conservation of a bulky hydrophobic residue situated at the face of the nicotinamide ring distal to the substrate. Some 10 years ago, Almarsson and Bruice [7] carried out MD studies of enzymatic substrate reductions with NAD(P)H. Attention was drawn to the positioning of bulky substituents at the NAD(P)H cofactor surface distal to the substrate [ILE 249 and VAL136 (1LDM [8]) for dogfish muscle lactate dehydrogenase; PHE103 (3DFR [9]) for dihydrofolate dehydrogenase; ALA245 and LEU157 (4MDH [10]) for malate dehydrogenase; and ILE12 and TYR317 (1GPD [11]) for glyceraldehydes 3-P dehydrogenase]. They noted that the steric demand of the bulky distal substituents induces the formation of one of two quasi-boat conformers of NAD(P)H in which the axial C4-H of NAD(P)H is pointed to the substrate carbonyl carbon and at times at van der Waals distance. The quasi-boat conformation contributes to the energetic advantage of enzymatic catalysis and is a required geometry along the pathway to the transition state [7,12–15]. Val203 is the conserved residue of HLADH [16]. The influence of Val203 on the dynamics of the E·S ground state can be appreciated when observing the molecular dynamics (MD) simulation of the HLADH· PhCHO·NADH complex [13]. The steric demand of Val203 induces an anisotropic bending of the dihydronicotinamide ring of NADH to a quasi-boat conformation with the hydrogen to be transferred in the axial position facing the substrate.

The enzyme residue Val203 was shown to be of particular importance in the early kinetic isotope effects studies of HLADH and mutants in the laboratories of Klinman [17] and in the steady-state kinetic studies of the same by Plapp [18].

* Corresponding author. Tel.: +1 805 893 2044; fax: +1 805 893 4120.
E-mail address: tcbruice@chem.ucsb.edu (T.C. Bruice).

0301-4622/$ - see front matter © 2006 Elsevier B.V. All rights reserved.
doi:10.1016/j.bpc.2006.05.009

Kinetic parameters and isotope effects, measured for a group of site-directed mutants of HLADH with benzyl alcohol as substrate, have shown that alterations of the single amino acid Val203 profoundly influences the degree of hydrogen tunneling [17]. Reduction in the size of the bulky amino acid side chain (Val203) results in a decrease in the rate of reaction. The log (k_{cat}/K_M) decreases in a linear fashion with an increase in the MD-derived closest contact distance (CCD) between reactants in wild-type (VAL203) and mutant (V203L, V203A, and V203G) forms in single 203-position mutant structures [13] (Eq. (3)):

$$Log(k_{cat}/K_M) = -1.63\ \mathrm{CCD} + 6.65 \quad (3)$$

Thus, restriction of distance between reactants facilitates quantum mechanical tunneling. The bulky substituents thus promote near attack conformers (NACs). This distance was shown with HLADH·NAD^+·$PhCH_2O^-$ complex to be diminished by anti-correlation motions of the enzyme structure, which create push-NACs [19]. Four pairs of anti-correlated interactions at the active site were identified. The motions of Cα of Val292 and CG1 of Val203 in the cofactor binding domain towards C7 of $PhCH_2O^-$ are most important in the ~0.5 Å pushing of reactant atoms (C4 of NAD^+ towards C7 of $PhCH_2O^-$) to form push-NACs [19]. The reactant atoms are at van der Waals distance and the angle of approach is between 132° and 180° [4]. Additionally, the ground-state NAC species had been shown to be associated with the transition states of lowest energy [19].

Colonna-Cesari et al. [20] reported inter-domain motion in liver alcohol dehydrogenase, calculated for the apo- and holoenzymes by use of empirical energy functions, that showed that the motion for the catalytic domain around a calculated axis is of a sliding type; the catalytic domain rotates relative to the coenzyme-binding domain while moving closer to it. These reported sliding and rotation motions about the catalytic domain around the hinge axes and towards the coenzyme-binding domain traverse the active site and result in the anti-correlated motions for the portions of the two domains. Ten-nanosecond MD and cross-correlation analysis of the HLADH·NAD^+·$PhCH_2O^-$ complex by Luo et al. [21] had established anti-correlated motions between the NAD^+ binding domain and other portions of the enzyme [21].

In this study we are interested in isolating those residues and/or portions of the enzyme that participate in functionally important structural rearrangement in terms of domain motions and their specific directions of collective motions based on normal mode analyses. Normal mode analysis (NMA) is a method for studying long-time dynamics and elasticity of biological systems. Many studies have shown that the results from NMA can provide a propder description of the functionally important motions of proteins [22–35].

2. Methods

Normal mode analysis was performed using the elastic network model [36] applying the single-parameter Hookean potential [37] and protein models. Several studies have shown that a single parameter potential is sufficient to reproduce complex slow dynamics in good detail [29,35–37]. Moreover, the elastic network model provides an efficient way to study the characteristics and directions of low-frequency motions. A lot of information about the nature of the large conformational changes of biological systems can be obtained from a single normal mode. For example, a single low-frequency normal mode can be found whose direction compares well with the conformational change or gives a good description of the pattern of the atomic displacement as observed experimentally. The single-parameter Hookean potential [37] was also tested, using an all-atom model, on a periplasmic maltodextrin binding protein. The results indicated that the slowest modes closely map the open form going to the closed form [37].

In our elastic network model, the protein residues are represented by their Cα atoms. To reduce space requirements, 74 residues from the C-terminal were removed, leaving 300 residues. A Hessian matrix was constructed using a force constant of 1 kJ $Å^{-2}$ mol^{-1} and a cutoff of 8 Å. The figures showing the normal mode vectors were generated using the VMD program [38].

3. Results and discussion

Three normal modes (mode 1, mode 7, and mode 8, after the six trivial translation and rotation modes were removed) in the lowest frequency region will be discussed here. These three modes of motions represent most characteristics in the large domain motions of the enzyme from 20 lowest frequency modes carefully examined. Fig. 1A shows an overall picture of the enzyme interaction in the lowest frequency mode (mode 1). Each arrow in black represents the vector of motion of a Cα atom. The enzyme residues are omitted for easier viewing. The substrate and the cofactor (coenzyme) are shown as sticks. In Fig. 1a, the vectors of the large catalytic domain (right, residues 1–175) and the coenzyme-binding domain (left, residues 176–300) collectively form two qualitative circles moving towards the active site pocket and merge at an angle by sliding into each other.

Fig. 1B and C provides an enlarged local view of Fig. 1A with the vectors pointing towards the coenzyme's nicotinamide ring (left) or the substrate $PhCH_2O^-$ (right). The Cα atoms of these residues are shown as color-coded balls in Fig. 1b or c. The vectors for residues Pro91, Leu92, Phe93, Thr94, Lys113, Asn114 Asp115 Leu116, Ser117, and Leu141 collectively point towards the substrate alcohol from the upper right, and the vectors for residues Ser177, Thr178, Gly179, Tyr180, Gly181, Ser182, Ala183, Val184, Lys185, Val186, Ala187, Lys188, Val207, Phe266, Glu267, Val290, Ile291, and Val292 collectively point towards the coenzyme's nicotinamide ring from the lower left.

In Fig. 1B, the residue Val292 (green) is situated at the face of the nicotinamide ring distal to substrate alcohol and is in position to push the nicotinamide ring towards the substrate alcohol [19]. Normal mode analysis further shows that in the

lowest frequency normal mode the vector of Val292 points directly towards the nicotinamide ring. Residue V292 was also identified as important in experimental mutants steady state and transient kinetics studies [18], involving anti-correlated motions in pushing the reactants [19] and creating a protein-promoting vibration in the reaction catalyzed by HLADH [39–41].

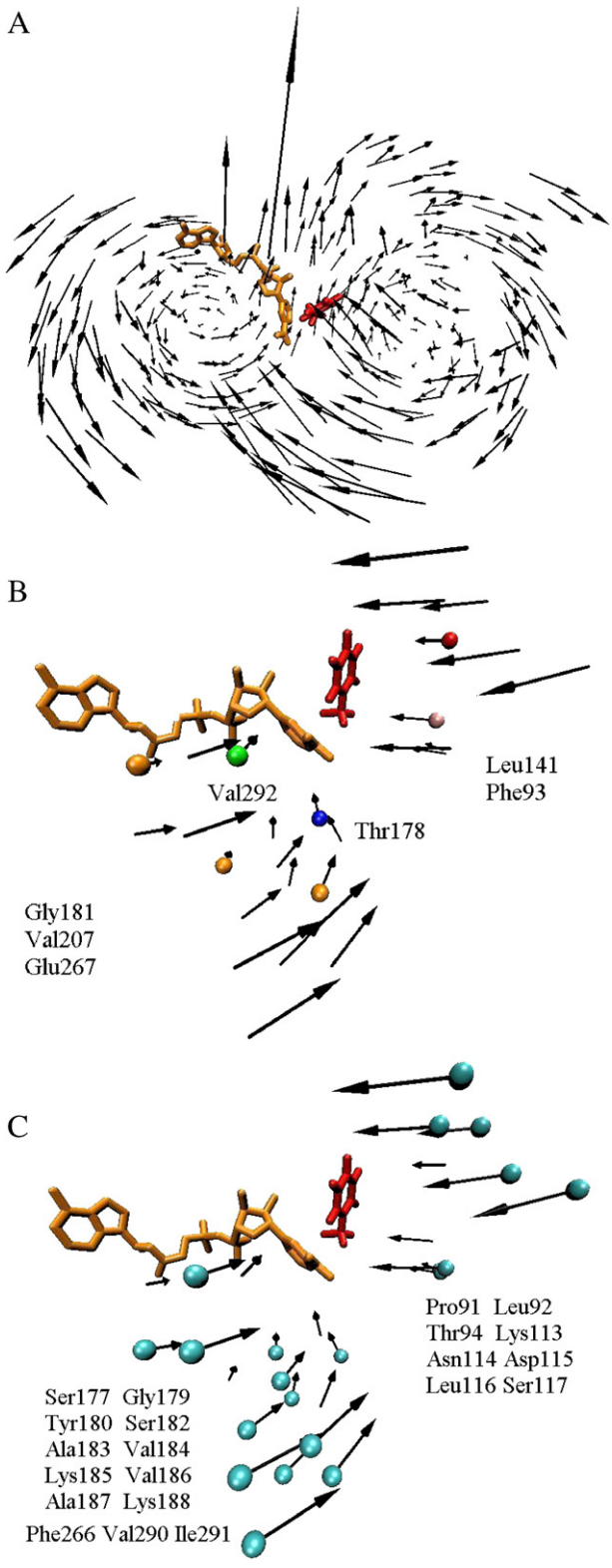

Fig. 1. (A) An overall picture of the lowest frequency mode (mode 1). Each arrow in black represents the vector of motion of a Cα atom. The enzyme residues are omitted for easier viewing. The substrate (red) and the cofactor (orange) are shown as sticks. (B) An enlarged local view of (A) with the vectors pointing towards the coenzyme's nicotinamide ring (left) or the substrate $PhCH_2O^-$ (right). The Cα atoms of a portion of these residues are shown as color-coded balls. The residue Val292 (green) is situated at the face of the nicotinamide ring distal to substrate alcohol, and the vector of Val292 points directly towards the nicotinamide ring. The residue Thr178 (dark blue) is situated at the side of the nicotinamide ring, and the vector of Thr178 points towards the nicotinamide ring. The vector of residue Leu141 (red) points towards the substrate. The vectors of residues Gly181, Val207, and Glu267 (orange) located at the far left are within the collective motions to push the nicotinamide ring from the coenzyme-binding domain towards the substrate. The pink-colored Cα atom and its vector show the position and the direction of residue Phe93. (C) An enlarged local view of (A) with the vectors pointing towards the coenzyme's nicotinamide ring (left) or the substrate $PhCH_2O^-$ (right). The Cα atoms of a portion of these residues are shown as color-coded balls. The residues Pro91, Leu92, Thr94, Lys113, Asn114, Asp115, Leu116, and Ser117 in cyan are within the collective motions to push the substrate from the catalytic domain towards the nicotinamide ring from the upper right; and the residues Ser177, Gly179, Tyr180, Ser182, Ala183, Val184, Lys185, Val186, Ala187, Lys188, Phe266, Val290, and Ile291 in cyan are within the collective motions to push the nicotinamide ring from the lower left. (For interpretation of the references to colour in this figure legend, the reader is referred to the web version of this article.)

The residue Thr178, in dark blue (Fig. 1B), is situated at the side of the nicotinamide ring, and in position to push the nicotinamide ring from the side [19]. Normal mode analysis further shows that the vector of Thr178 points towards the nicotinamide ring. Residue Thr178 was also identified as important in experimental mutants steady-state and transient kinetics studies [18] and involving anti-correlated motions in pushing the reactants [19].

The residue Leu141 (red), at the far right (Fig. 1B), is in a position to push the substrate alcohol towards the nicotinamide ring from the upper right [19]. Normal mode analysis further shows that the vector of Leu141 points towards the substrate. Residue Leu141 was identified with Thr178 as an anti-correlated pair pushing the reactants [19].

The vectors of residues Gly181, Val207, and Glu267 (orange) located at the far left (Fig. 1B) are within the collective motions to push the nicotinamide ring from the coenzyme-binding domain towards the substrate. Residues Gly181, Val207, and Glu267 were also identified as creating a protein-promoting vibration in the reaction catalyzed by HLADH by Mincer et al. and Caratzoulas et al. [39–41].

Residue Phe93 (pink), located at the lower right of Fig. 1b, is in position to push the substrate towards the nicotinamide ring from the upper right. In a kinetic isotope effects study, residues Phe93 and Leu57 were used to design site-directed mutations in an effort to "unmask" tunneling [5]. The reduction in the size of the alcohol-binding pocket through substitution at residues 57 and 93, which are in van der Waals contact with bound alcohol produced a clear demonstration of protium tunneling. The pink-colored Cα atom and its vector show the position and the direction of residue Phe93.

In Fig. 1C, the residues Pro91, Leu92, Thr94, Lys113, Asn114, Asp115, Leu116, and Ser117 in cyan are within the collective motions to push the substrate from the catalytic

domain towards the nicotinamide ring from the upper right; and the residues Ser177, Gly179, Tyr180, Ser182, Ala183, Val184, Lys185, Val186, Ala187, Lys188, Phe266, Val290, and Ile291 in cyan are within the collective motions to push the nicotinamide ring from the lower left.

Fig. 2A shows an overall picture of the enzyme interaction in mode 8. Each arrow in black represents the vector of motion of an Cα atom. The enzyme residues are omitted for easier viewing. The substrate and the cofactor (coenzyme) are shown as sticks. In Fig. 2A, most of the vectors of the coenzyme-binding domain (left, residues 176–300) collectively point towards the active site, except those at the top and the left of the figure, which point away from the active site. A large potion of vectors in the large catalytic domain (right, residues 1–175) collectively point towards the active site, except some at the back right and the lower portion, which point away from the active site. There are a substantial number of vectors in the lower left of the coenzyme-binding domain with the direction to "push" upright to the coenzyme. There are a similar number of vectors in the upper right of the catalytic domain with the direction to "push" the alcohol substrate into the coenzyme nicotinamide ring region. The outwards enlarging tendency of the rest of the residues suggests their readiness to assist the product to move out of the reaction pocket.

Fig. 2B and C provides an enlarged local view of Fig. 2A with the vectors pointing towards the coenzyme's nicotinamide ring or the substrate alcohol. The Cα atoms of these residues are shown as color-coded balls in Fig. 2B or C. The vectors for residues Asp115, Pro119, Arg120, Gly121, Thr122, Met123, His138, His139, Phe140, and Leu141 collectively point towards the substrate from the upper right; and the vectors for residues Gly202, Val203, Gly204, Leu205, Ser206, Val207, Lys231, Ala232, Lys233, Glu234, Val235, Gly236, and Ala237 collectively point towards the coenzyme's nicotinamide ring from the lower left.

In Fig. 2B, the residue Val203 (green) is situated at the face of nicotinamide ring distal to the substrate, and in position to push the nicotinamide ring towards the substrate [19]. Normal mode analysis further shows that in mode 8 the vector of Val203 points directly towards the nicotinamide ring. Residue V203 was identified as also important in experimental kinetics studies [17,18], involving anti-correlated motions in pushing the reactants together [19], and creating a protein-promoting vibration in the reaction catalyzed by HLADH [39–41].

In Fig. 2B, the residue Leu141 (red) at the right is in a position to push the substrate towards the nicotinamide ring

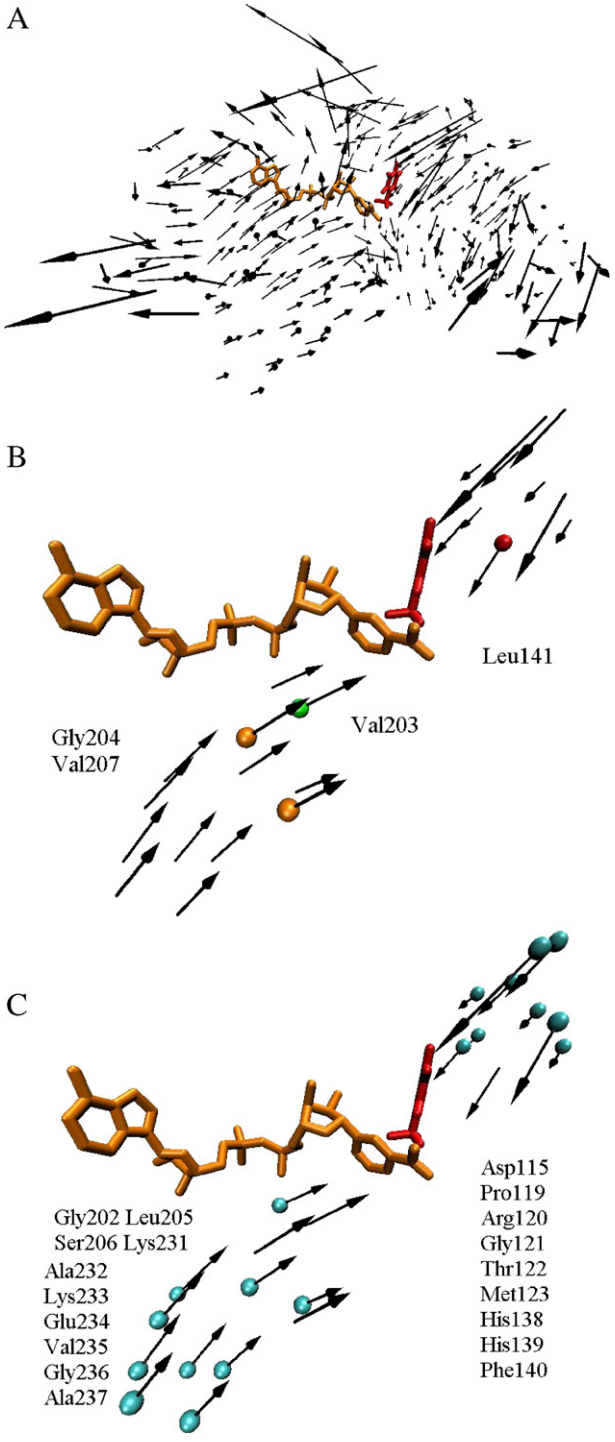

Fig. 2. (A) An overall picture of the mode 8. Each arrow in black represents the vector of motion of a Cα atom. The enzyme residues are omitted for easier viewing. The substrate (red) and the cofactor (orange) are shown as sticks. (B) An enlarged local view of (A) with the vectors pointing towards the coenzyme's nicotinamide ring or the substrate alcohol. The Cα atoms of a portion of these residues are shown as color-coded balls. The residue Val203 (green) is situated at the face of nicotinamide ring distal to the substrate, and the vector of Val203 points directly towards the nicotinamide ring. The residue Leu141 (red) at the right points to the substrate. The residues Gly204 and Val207 (orange) at the lower left are within the collective motions to push the nicotinamide ring towards the substrate from the lower left. (C) An enlarged local view of (A) with the vectors pointing towards the coenzyme's nicotinamide ring or the substrate alcohol. The Cα atoms of a portion of these residues are shown as color-coded balls. The residues Asp115, Pro119, Arg120, Gly121, Thr122, Met123, His138, His139, and Phe140 (cyan) located at the upper right are within the collective motions to push the substrate; and residues Gly202, Leu205, Ser206, Lys231, Ala232, Lys233, Glu234, Val235, Gly236, and Ala237 (cyan) located at the lower right are within the collective motions to push the nicotinamide ring. (For interpretation of the references to colour in this figure legend, the reader is referred to the web version of this article.)

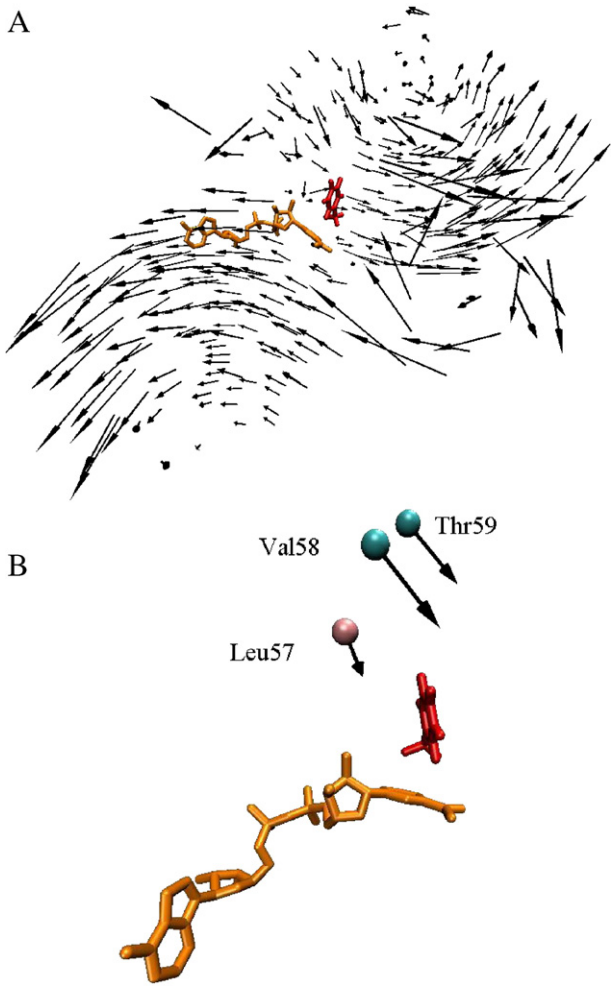

Fig. 3. (A) An overall picture of the mode 7. (B) An enlarged local view of (A). The pink-colored Cα atom and its vector show the position and direction of residue Leu57. The residue Leu57 in pink, the residues Val58 and Thr59 in cyan, located above the Leu57, are pointing towards the substrate from the upper left side. (For interpretation of the references to colour in this figure legend, the reader is referred to the web version of this article.)

from the upper right [19]. Only residue Leu141 showed up in this mode as functionally relevant from the reported anti-correlated Thr178 and Leu141 pair [19]. Residue Leu141 also appears pointing towards the substrate in the previous described lowest frequency mode.

Residues Gly204 and Val207 (orange) at the lower left (Fig. 2B) are within the collective motions to push the nicotinamide ring towards the substrate from the lower left. Residues Gly204 and Val207 were also identified as creating a protein-promoting vibration in the reaction catalyzed by HLADH [39–41]. The residue Val207 also appeared pointing towards the nicotinamide ring in the lowest frequency mode (mode 1) described previously.

In Fig. 2C, the residues Asp115, Pro119, Arg120, Gly121, Thr122, Met123, His138, His139, and Phe140 (cyan) located at the upper right are within the collective motions to push the substrate from the catalytic domain towards the nicotinamide ring from the upper right; and residues Gly202, Leu205, Ser206, Lys231, Ala232, Lys233, Glu234, Val235, Gly236, and Ala237 (cyan) located at the lower right are within the collective motions to push the nicotinamide ring from the lower left. These residues are identified as functionally important in the current study.

Fig. 3A shows an overall picture of the enzyme interaction in mode 7. In Fig. 3A, the vectors of the large catalytic domain (right, residues 1–175) and the coenzyme-binding domain (left, residues 176–300) are qualitatively anti-correlated and collectively sliding away from each other. This mode may facilitate the reaction product to be released. Fig. 3B provides an enlarged local view of Fig. 3A. The pink-colored Cα atom and its vector show the position and direction of residue Leu57. Leu57 and Phe93 were studied by the isotope effects study [5]. The residue Leu57 in pink, the residues Val58 and Thr59 in cyan, located above the Leu57 are pointing towards the substrate from the upper left side. These three residues are in position to assist the reaction product release.

NMA using the elastic network model applied in this study has provided characteristics and directions of the low-frequency large domain motions. The pattern of the atomic displacement revealed in this study is in line with experimental structural and kinetic studies [2,17,18] and theoretical simulations [19–21,39–41]. While the large domain motions are within the low-frequency time scale detectable by NMR technology, the anti-correlated motions and protein-promoting vibrations are at the picosecond to nanosecond time range. While the higher frequency motions promote the NACs formation, the lower frequency motions are domain motions in nature that bring the reactants together/apart.

Acknowledgment

This work was supported by a grant from the National Institutes of Health (5R37DK09171).

References

[1] C.I. Brändén, H. Jörnvall, H. Eklund, B. Furugren, in: P.D. Boyer (Ed.), The Enzymes, vol. 11, Academic Press, NY, 1975, p. 103.
[2] S. Ramaswamy, H. Eklund, B.V. Plapp, Structures of horse liver alcohol dehydrogenase complexed with, NAD^+ and substituted benzyl alcohols, Biochemistry 33 (1994) 5230–5237.
[3] H. Eklund, B.V. Plapp, J.-P. Samama, C.I. Brändén, Binding of substrate in a ternary complex of horse liver alcohol dehydrogenase, J. Biol. Chem. 23 (1982) 14349–14358.
[4] J. Luo, T.C. Bruice, Dynamic structures of horse liver alcohol dehydrogenase (HLADH): results of molecular dynamics simulations of HLADH–NAD^+–$PhCH_2OH$, HLADH–NAD^+–$PhCH_2O^-$, and HLADH–NADH–PhCHO, J. Am. Chem. Soc. 123 (2001) 11952–11959.
[5] B.J. Bahnson, D.-H. Park, K. Kim, B.V. Plapp, J.P. Klinman, Unmasking of hydrogen tunneling in the horse liver alcohol dehydrogenase reaction by site-directed mutagenesis, Biochemistry 32 (1993) 5503–5507.
[6] J.P. Klinman, in: P.F. Cook (Ed.), Enzyme Mechanism for Isotope Effects, CRC Press, Boca Raton, FL, 1991, p. 127.
[7] Ö. Almarsson, T.C. Bruice, Evaluation of the factors influencing reactivity and stereospecificity in NAD(P)H dependent enzymes, J. Am. Chem. Soc. 115 (1993) 2125–2138.
[8] C. Abad-Zapatero, J.P. Griffith, J.L. Sussman, M.G. Rossmann, Refined crystal structure of dogfish M_4 apo-lactate dehydrogenase, J. Mol. Biol. 198 (1987) 445.

[9] D.J. Filman, J.T. Bolin, D.A. Matthews, J. Kraut, Crystal structures of *Escherichia coli* and *Lactobacillus casei* dihydrofolate reductase refined at 1.7 Å resolution, J. Biol. Chem. 257 (1982) 13663.
[10] J.J. Birktoft, G. Rhodes, L.J. Banascak, Refined crystal structure of cytoplasmic malate dehydrogenase at 2.5-Å resolution, Biochemistry 28 (1989) 6065.
[11] D. Moras, K.W. Olson, M.N. Sabesan, M. Buehner, G.C. Ford, M.G. Rossmann, Studies of asymmetry in the three-dimensional structure of lobster D-glyceraldehyde-3-phosphate dehydrogenase, J. Biol. Chem. 250 (1975) 9137.
[12] Ö. Almarsson, A. Sinha, E. Gopinath, T.C. Bruice, Mechanism of one-electron oxidation of NAD(P)H and function of NADPH bound to catalase, J. Am. Chem. Soc. 115 (1993) 7093–7102.
[13] J. Luo, K. Kahn, T.C. Bruice, The linear dependence of $\log(k_{cat}/K_m)$ for reduction of NAD^+ by $PhCH_2OH$ on the distance between reactants when catalyzed by horse liver alcohol dehydrogenase and 203 single point mutants, Bioorganic Chem. 27 (N4) (1999) 289–296.
[14] M. Garcia-Viloca, C. Alhambra, D.G. Truhlar, J. Gao, Inclusion of quantum-mechanical vibrational energy in reactive potentials of mean force, J. Chem. Phys. 114 (2001) 9953–9958.
[15] K. Beis, S.T.M. Allard, A.D. Hegeman, G. Murshudov, D. Philip, J.H. Naismith, The structure of NADH in the enzyme dTDP-D-glucose dehydratase (RmlB), J. Am. Chem. Soc. 125 (2003) 11872–11878.
[16] H.-W. Sun, B.V. Plapp, Progressive sequence alignment and molecular evolution of the Zn-containing alcohol dehydrogenase family, J. Mol. Evol. 34 (1992) 522–535.
[17] B.J. Bahnson, T.D. Colby, J.K. Chin, B.M. Goldstein, J.P. Klinman, A link between protein structure and enzyme catalyzed hydrogen tunneling, Proc. Natl. Acad. Sci. U. S. A. 94 (1997) 12797–12802.
[18] J.K. Rubach, B.V. Plapp, Amino acid residues in the nicotinamide binding site contribute to catalysis by horse liver alcohol dehydrogenase, Biochemistry 42 (2003) 2907–2915.
[19] J. Luo, T.C. Bruice, Anticorrelated motions as a driving force in enzyme catalysis: the dehygrogenase reaction, Proc. Natl. Acad. Sci. U. S. A. 101 (2004) 13152–13156.
[20] F. Colonna-Cesari, D. Perahia, M. Karplus, H. Eklund, C.I. Brändén, O. Tapia, Interdomain motion in liver alcohol dehydrogenase, J. Biol. Chem. 261 (1986) 15273–15280.
[21] J. Luo, T.C. Bruice, Ten-nanosecond molecular dynamics simulation of the motions of the horse liver alcohol dehydrogenase $PhCH_2O^-$ complex, Proc. Natl. Acad. Sci. U. S. A. 99 (2002) 16597–16600.
[22] N. Go, T. Noguti, T. Nishikawa, Dynamics of a small globular proteins in terms of low-frequency vibrational modes, Proc. Natl. Acad. Sci. U. S. A. 80 (1983) 3696–3700.
[23] B. Brooks, M. Karplus, Harmonic dynamics of proteins: normal mode and fluctuations in bovine pancreatic trypsin inhibitor, Proc. Natl. Acad. Sci. U. S. A. 80 (1983) 6571–6575.
[24] M. Levitt, C. Sander, P.S. Stern, Protein normal-mode dynamics: trypsin inhibitor, crambin, ribonuclease and lysozyme, J. Mol. Biol. 181 (1985) 423–447.
[25] J.F. Gibrat, N. Go, Normal mode analysis of human lysozyme: study of the relative motion of the two domains and characterization of the harmonic motion, Proteins 8 (1990) 258–279.
[26] O. Marques, Y.H. Sanejouand, Hinge-bending motion in citrate synthase arising from normal mode calculations, Proteins 23 (1995) 557–560.
[27] H. Wako, M. Tachikawa, A. Ogawa, A comparative study of dynamic structures between phage 434 cro and repressor proteins by normal mode analysis, Proteins 26 (1996) 72–80.
[28] A. Thomas, M.J. Field, D. Perahia, Analysis of the low frequency normal modes of the T-state of aspartate transcarbamylase, J. Mol. Biol. 257 (1996) 1070–1087.
[29] K. Hinsen, Analysis of domain motions by approximate normal mode calculations, Proteins 33 (1998) 417–429.
[30] A. Kitao, N. Go, Investigating protein dynamics in collective coordinate space, Curr. Opin. Struck. Biol. 9 (1999) 164–169.
[31] D.W. Miller, D.A. Agard, Enzyme specificity under dynamic control: a normal mode analysis of α-Lytic protease, J. Mol. Biol. 286 (1999) 267–278.
[32] H. Kikuchi, H. Wako, K. Yura, M. Go, M. Mimuro, Significance of a two-domain structure in subunits of phycobiliproteins revealed by the normal mode analysis, Biophys. J. 79 (2000) 1587–1600.
[33] H.J.C. Berendsen, S. Hayward, Collective protein dynamics in relation to function, Curr. Opin. Struck. Biol. 10 (2000) 165–169.
[34] P. Chacon, F. Tama, W. Wriggers, Mega-Dalton biomolecular motion captured from electron microscopy reconstructions, J. Mol. Biol. 326 (2003) 485–492.
[35] F. Tama, M. Valle, J. Frank, C.L. Brooks III, Dynamic reorganization of the functionally active ribosome explored by normal mode analysis and cryo-electron microscopy, Proc. Natl. Acad. Sci. U. S. A. 100 (2003) 9319–9323.
[36] F. Tama, Y.-H. Sanejouand, Conformational change of proteins arising from normal mode calculations, Protein Eng. 14 (2001) 1–6.
[37] M.M. Tirion, Large amplitude elastic motions in proteins from a single-parameter, atomic analysis, Phys. Rev. Lett. 77 (1996) 1905–1908.
[38] W. Humphrey, A. Dalke, K. Schulten, VMD: visual molecular dynamics, J. Mol. Graph. 14 (1996) 33–38.
[39] J.S. Mincer, S.D. Schwartz, Protein promoting vibrations in enzyme catalysis—A conserved evolutionary motif, J. Proteome Res. 2 (2003) 437–439.
[40] S. Caratzoulas, J.S. Mincer, S.D. Schwartz, Identification of a protein-promoting vibration in the reaction catalyzed by horse liver alcohol dehydrogenase, J. Am. Chem. Soc. 124 (2002) 3270–3276.
[41] J.S. Mincer, S.D. Schwartz, A computational method to identify residues important in creating a protein promoting vibration in enzymes, J. Phys. Chem., B 107 (2003) 366–371.